JST: Engineering and Technology for Sustainable Development
Volume 33, Issue 2, April 2023, 022-028

Hydrothermal Synthesis of Nanostructured V_2O_5 Material for Photocatalytic Applications: Effect of Surfactants

Do Quang Dat[1,2], Chu Manh Hung[2], Nguyen Van Duy[2], Lam Van Nang[1*], Vo Thi Lan Phuong[1], Le Thi Minh Ngoc[1], Tran Ngoc Tu[1], Pham Thi Nga[1] Nguyen Thiet Ke[1], Lai Van Duy[2], Nguyen Duc Hoa[2]

[1]*Department of Natural Sciences, Hoa Lu University, Ninh Binh, Vietnam*
[2]*International Institute for Materials Science, Hanoi University of Science and Technology, Ha Noi, Vietnam*
[*]*Corresponding author email: lvnang@hluv.edu.vn*

Abstract

In the study, the nanostructured V_2O_5 photocatalyst was prepared by a hydrothermal process followed by calcination with the addition of various surfactants to the precursor solution. The synthesized V_2O_5 nanomaterials were investigated by scanning electron microscopy (SEM), X-ray diffraction (XRD), Fourier transform infrared spectra (FTIR), and ultraviolet - visible spectroscopy (UV-vis). The SEM images and XRD spectra showed that the V_2O_5 nanomaterials with different morphologies crystallized in the orthorhombic phase were successfully synthesized. The FTIR spectrum gives characteristic oscillations of the chemical bonds in V_2O_5, containing the V-O-V vibration. The UV-Vis spectrum determines the band gap energy in accordance with the bandgap energy value of V_2O_5. In particular, the results demonstrated that the addition of surfactant had a strong effect on the morphology, band gap energy and surface chemistry of the photocatalysts. The comparison between the addition of the three surfactants of dodecyl sulfate sodium, pluronic P123, and CTAB showed that the addition of SDS produced the most efficient V_2O_5 photocatalyst is beneficial to improve V_2O_5 agglomeration. Under the illumination of the Compact lamp, the V_2O_5 product using SDS removal could reach up to 90% Methylene Blue solution after 120 minutes.

Keywords: Vanadium pentoxide, nanostructures, photocatalyst, hydrothermal, surfactant.

1. Introduction

The textile industry is one of the most important sectors of the global economy, and the twenty-first century is known as the "Industry 4.0 century," with all its innovations and achievements. The rapid expansion of the textile industry is harmful to the environment, particularly the wastewater produced by the cooking, bleaching, and dyeing processes [1]. Water contains complex colour-carrying groups as well as long-lasting organic compounds, which are especially important during the dyeing process. As a result, their waste pollutes the environment, harms aquatic life, and is carcinogenic to both humans and animals. Numerous physical, chemical, and biological techniques have been employed to date to remove a variety of pollutants from wastewater. One of these approaches, semiconductor photocatalytic oxidation, has been researched as one of the most cutting-edge and eco-friendly ways to treat organic pollutants.

Vanadium oxide (V_2O_5), a transition metal oxide semiconductor with a narrow band gap (2.5 eV), is an excellent candidate for capturing visible, UV, and sunlight light. A significant portion of the solar spectrum can be captured and used to build active redox centers. However, its ability to photodegrade pollutants efficiently is limited by the rapid recombination of photo-excited electron/hole (e^-/h^+) pairs and a small specific surface area.

Recently, V_2O_5 nano and microstructures have been extensively studied with their advantageous properties (optical, structural, mechanical, and biological) due to their high specific surface area, layered structure, low cost, low toxicity, abundance in nature, ect. In the application of photocatalysts, V_2O_5 is of great interest because of its unique advantages: narrow band gap, reactivity in the visible light region, high efficiency, chemical stability, etc. It might be one of the best-suited catalyst materials for photocatalytic application. A variety of V_2O_5 nanostructures, such as nanourchins, nanotubes, nanospikes, nanorods, nanowires, and nanobelts have been prepared by using the most popular synthesis techniques include sol-gel, hydrothermal, solid-state reaction, etc. [1, 2]. Furthermore, the photocatalytic activity of V_2O_5 is believed to be strongly dependent on the morphology, surface area and band gap energy because the photocatalytic reaction occurs at the catalyst surface in the dye solution under the radiation of the light. There are many factors in the synthesis process that directly affect the morphology and surface of the catalyst such

ISSN 2734-9381
https://doi.org/10.51316/jst.165.etsd.2023.33.2.4
Received: February 7, 2023; accepted: March 22, 2023

as: pH, temperature, precursor content, surfactant, etc. Among them, the use of surfactants is influenced the morphology of the fabricated materials as they reduce the energy and surface tension of the particles thereby minimizing the agglomeration of the nanostructures. Aslam, *et al.* synthesized V_2O_5 by chemical precipitation procedure using Triton X-100 as morphology mediator under sunlight for the degradation of phenol and their derivatives [3]. Raj *et al.* prepared Vanadium pentoxide crystalline nanoparticles hydrothermally in the presence of various surfactants named Sodium Dodecyl Sulphate (SDS), Cetyl Trimethyl Ammonium Bromide (CTAB) and Triton-X. The photocatalytic studies were performed and found better photocatalytic efficiency in V_2O_5 prepared with SDS, obtained through the degradation of MO dye under UV light irradiation [4]. I. Ibrahim, *et al*. synthesized V_2O_5 by wet chemical process using four different surfactants PVP, SDS, T100 and T80 and then compared their photocatalytic performance. The results showed that, under UV light, the most efficient photocatalyst (T80) was based on Tween 80 surfactant capable to reduce hexavalent chromium to trivalent by up to 70% and showed high yield in the decomposition of methylene blue and tetracycline antibiotic water pollutants [5].

In general, studies of the effects of the surfactants on the synthesis process, the characterization and the photocatalytic activity of the V_2O_5 nano/microstructures is rare and it is an potential area. In this study, different V_2O_5 nanostructures were successfully synthesized using different surfactants (P123, SDS and CTAB) by hydrothermal method followed by calcination. The photocatalytic properties of Methylene Blue solution decomposition of all V_2O_5 products under visible light were compared and analysed.

2. Experiment

2.1. Fabrication of V_2O_5 Nanostructures

The following chemicals were used: ammonium metavanadate (NH_4VO_3, 99.99%), Poly(ethylene glycol)-block-poly(propylene glycol)-block-poly(ethylene glycol) (Pluronic P-123, $HO(CH_2CH_2O)_{20}(CH_2CH(CH_3)\ O)_{70}(CH_2CH_2O)_{20}H$, 99%), Cetrimonium bromide (CTAB, $[(C_{16}H_{33})N(CH_3)_3]Br$, 99%), Sodium dodecyl sulfate (SDS, $CH_3(CH_2)_{11}OSO_3Na$, 98.5%), hydrochloric acid (HCl), and ethanol (CH_3CH_2OH, 99.8%) were bought from Sigma-Aldrich. Deionized water was used as a solvent to prepare solution.

V_2O_5 nanostructures were synthesized by hydrothermal method. In a typical procedure, ammonium metavanadate [NH_4VO_3] (10 mmol) was dissolved in 60 mL of deionized water containing P123 under continuous stirring for 15 min. Then, 10 mL of hydrochloric acid [HCl (1M)] was slowly added into the above mixture stirring for another 30 min. The solution was then transferred to a 100 mL Teflon-lined stainless-steel autoclave for hydrothermal heating. The hydrothermal process was maintained at 200 °C for 24 h. After being gradually cooled to room temperature, the precipitate at the bottom was centrifuged and washed with deionized water several times. It was then also washed several times with ethanol solution and collected by centrifugation at 5800 rpm. The obtained blue-black powder was dried in an oven at 60 °C for 24 h, and then calcined at 500 °C/2h. The same method was followed to prepare V_2O_5 nanostrures from NH_4VO_3 using with other two surfactants CTAB and SDS (Fig. 1). The samples were labelled as V_2O_5-P123, V_2O_5-SDS, V_2O_5-CTAB, respectively. All three V_2O_5 samples were taken for characterization.

The synthesized materials were characterized by field-emission scanning electron microscopy (SEM – JEOL 7600), X-ray diffraction (XRD, X-Pert Pro, Malvern Panalytical Ltd., Malvern, UK) with a Cu-K_α source in a 2θ range from 10° to 90° and Optical absorption spectra (UV-vis) were investigated using an Ultraviolet - visible spectrometer (PG-T90, UK). FTIR spectra were measured on a Nexus 670-Nicole.

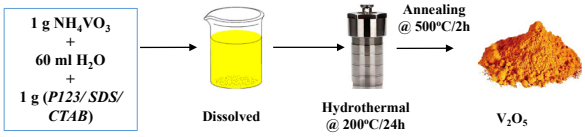

Fig. 1. Schematic of hydrothermal synthesis of V_2O_5 using different surfactants.

2.2. The Photocatalytic Activity of V_2O_5 Nanomaterials

The photocatalytic performance of V_2O_5 samples was investigated with Methylene Blue (MB) solution with initial concentration of 20 mg/l under irradiation of compact lamp (220 V, 120 W). Typically, experiments were conducted in a closed reactor house: 30 mg of V_2O_5 powder and 100 ml of MB solution (20 mg/l) were stirred in a 250 ml beaker using a magnetic stirrer in the dark for 60 min to achieve equilibrium adsorption between MB solution and V_2O_5 powder. Next, the system is illuminated with compact fluorescent lamp. The distance between the lamp and the beaker is about 15 cm. At specific time intervals, about 7 ml of the solution was withdrawn from the mixture and centrifuged to completely remove the catalyst. The solution was then analyzed using an ultraviolet-visible spectrophotometer. MB concentration was measured at λ_{max} = 664 nm.

3. Results and Discussions

3.1. SEM Analysis

Fig. 2 shows the morphology of three fabricated samples of V_2O_5 material depending on the different

surfactants used during hydrothermal synthesis. There are significant differences among the products. The V_2O_5-CTAB sample (Fig. 2a) is a leaf-rod nanostructures with a length of 1-2 µm, heterogeneously interwoven with each other. By changing CTAB by SDS, a significant morphological change occurred (Fig. 2b), V_2O_5 was produced with heterogeneous morphology and formed large-sized clusters. Finally, with the combination with surfactant P123, the V_2O_5 nanostructures produce nanorods with small diameter of about 100 nm, and about 1-2 µm in length (Fig. 2c). Thus, there is a clear dependence between the surfactant and the morphology of the products.

The following processes may account for the stacking of thin nanosheets of V_2O_5 during the hydrothermal process:

$$NH_4VO_3 \leftrightarrow NH_4^+ + VO_3^- \quad (1)$$

$$2VO_3 + H_2 \leftrightarrow V_2O_5 + H_2O \quad (2)$$

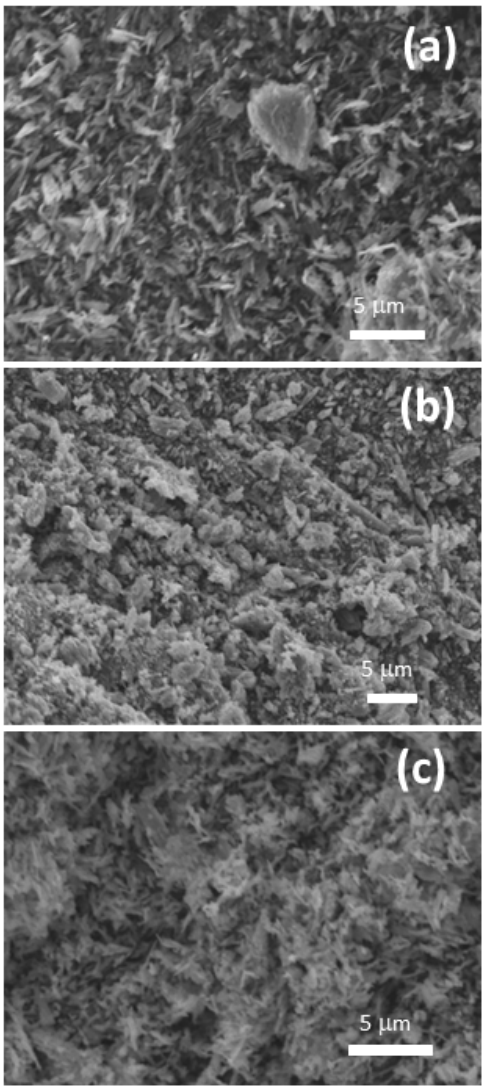

Fig. 2. SEM images of V_2O_5 samples prepared using SDS (a); CTAB (b) and P123 (c) surfactants.

In deionized water, NH_4VO_3, a precursor of Vanadium, has a propensity to split into NH^{4+} and VO_3^- ions. The addition of hydrochloric acid during synthesis raises the concentration of H^+ ions, which interact with the VO_3^- species to create V_2O_5. The production of thin nanosheets can be improved by the inclusion of the surfactant P123, CTAB, and SDS.

3.2. XRD Analysis

The crystal structure of the synthesized V_2O_5 samples was investigated using XRD measurement. Fig. 3 shows the XRD plot of the powder samples hydrothermally synthesized with different surfactants. It is found that all the peaks of all samples are pointed and sharp characteristic for the crystallization of the orthorhombic crystal structure V_2O_5 (JPDS card no 1-359) [6]. The most significant peaks typical in all samples are (001), (110) and (040). The highest intensity peak is (001) at a 2θ value of 20.4° indicating that the crystals grow preferentially in the ⟨001⟩ direction. In addition, no other additional peaks were found in the XRD pattern of all samples. Therefore, a high-purity V_2O_5 crystal structure with no impurities was synthesized by the addition of various surfactants.

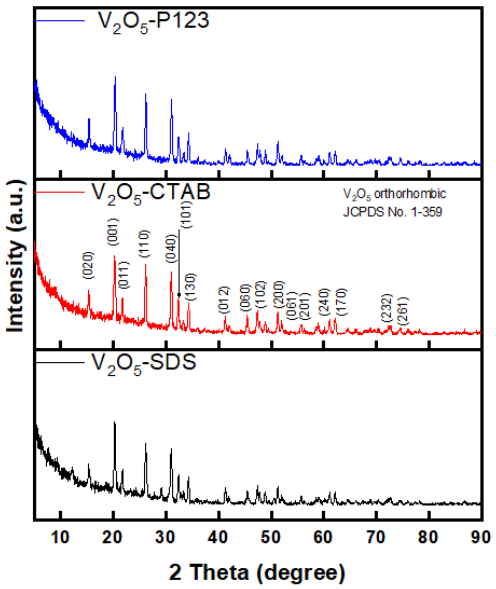

Fig. 3. XRD diagrams for V_2O_5 samples prepared using SDS, CTAB and P123 surfactants.

The size of the crystallite size obtained from the XRD pattern based on the Scherrer equation:

$$D = \frac{K\lambda}{\beta cos\theta} \quad (3)$$

where D is the average crystallite size (nm) of the samples, λ is the X-ray wavelength (nm), K is the constant, and θ and β-FWHM are the Bragg angle (rads) and the excess line broadening (rads), respectively. The average crystallite size (nm) was obtained using the Scherrer equation and presented in Table 1.

Table 1. The average crystallite size (nm) of the samples

Sample ID	Average crystallite size (nm)
V_2O_5-CTAB	57.187
V_2O_5-SDS	75.135
V_2O_5-P123	87.176

3.3. FTIR Analysis

Fig. 4 illustrates the FTIR spectra analysed in the range of 400 – 4000 cm^{-1} wave number of three V_2O_5 powder samples. It is found that here there are three dominant vibration bands belonging to the chemical bonds in V_2O_5 in all three material samples. Vibrations at wave numbers 477 and 589 cm^{-1} identified the symmetric stretching modes of V-O-V vibration [5, 7]. The observed peak around 1034 cm^{-1} is the vibration of the V = O bond with the terminal oxygen [8]. In addition, the peaks of 1381, 1627 cm^{-1} of small intensity representing the hydroxyl group can be observed and the peak at 3415 cm^{-1} is the vibration of the H-O-H bond, which means that there is still the presence of some water molecules in the products [9]. In addition, the peak appearance at wave number 2368 cm^{-1} is of CO_2 molecules absorbed on the surface. In the signal range, there were no peaks corresponding to the vibrations of the organic compounds, implying that the organic compounds of the precursors were completely decomposed after the annealing process. Therefore, FTIR analysis, in conjunction with XRD analysis, confirms the high purity of V_2O_5.

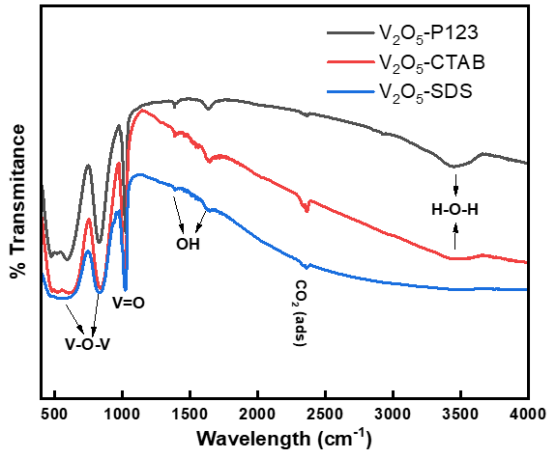

Fig. 4. FTIR spectra of V_2O_5 prepared samples using SDS; CTAB and P123 surfactants.

3.4. UV-Vis Analysis

Fig. 5 shows the effect of different surfactants on the absorption characteristics of the fabricated samples. On the UV-Vis spectrum of the four samples, it can be observed that the surfactants play an important role in changing the absorption characteristics of the sample (Fig. 5a). The samples all have high absorption in the ultraviolet light region. The band gap of V_2O_5 is calculated according to the following formula [7]:

$$E_g = h\nu - \frac{(\alpha h\nu)^{1/2}}{C} \quad (4)$$

where E_g is the band gap energy, $h\nu$ is the photon energy, α is the absorption coefficient, C is the energy dependent constant.

The bandgap energies of the V_2O_5 samples synthesized with different surfactants CTAB, SDS, P123 are 3.2, 2.8 and 2.2 eV, respectively (Fig. 5b). The reduction in the band gap energy is due to the ability of the individual surfactants to reduce the surface energy [1, 7]. Thus, surfactants play an important role in regulating the band gap energy of the product.

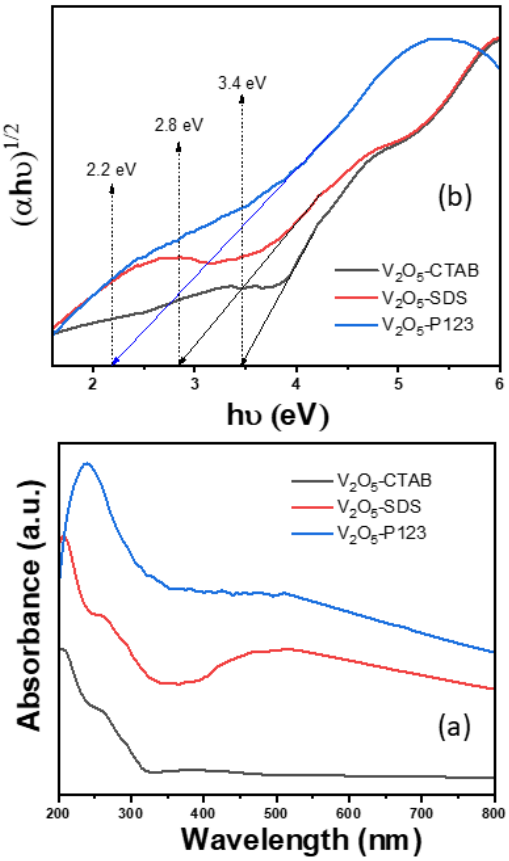

Fig. 5. UV-Vis spectra for V_2O_5-SDS, V_2O_5-CTAB and V_2O_5-P123 samples (a); respective Tauc plots and estimated band gaps of the synthesized materials (b).

3.5. Photodegradation of MB Solution under Visible Light Irradiation

The photocatalytic properties of MB solution decomposition using three V_2O_5 samples as catalysts

are shown in Fig. 6. The disappearance of the MB absorption peak at 664 nm after 2 h of illumination of all three experiments demonstrates that MB was degraded by V_2O_5 under the illumination of compact fluorescent lamp.

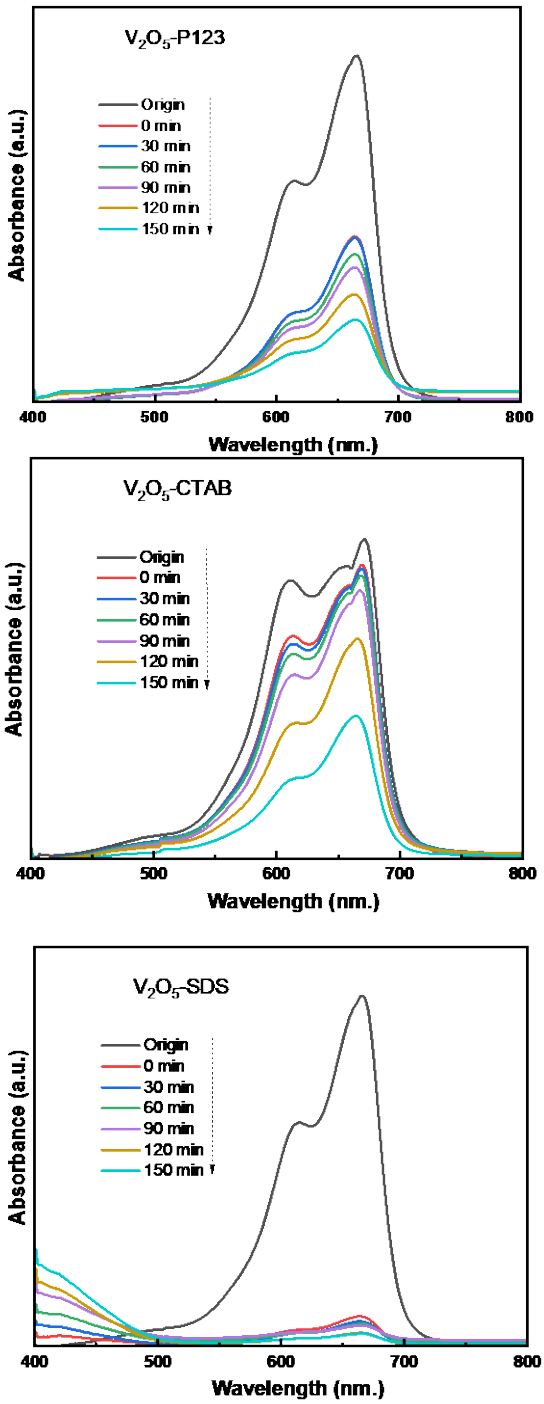

Fig. 6. UV–vis absorbance spectra of degraded MB using V_2O_5-SDS; V_2O_5-CTAB and V_2O_5-P123 nanostructures.

The photocatalytic decomposition efficiency of MB is determined according to the following equation:

$$H(\%) = \left(1 - \frac{C}{C_0}\right) \times 100\% \quad (5)$$

where H (%) is the decomposition efficiency, C_o is the origin concentration and C is the concentration at time t of the MB solution.

Fig. 7 compares the MB decolorization performance of the V_2O_5 samples. After 1 h of magnetic stirring in the dark, the V_2O_5 samples all adsorbed a little or most of the MB, in which, V_2O_5-SDS adsorbed up to 95%, V_2O_5-P123 adsorbed 50% and V_2O_5-CTAB adsorbed only about 5% amount of MB in solution. From 0 min to 180 min, under the illumination of compact lamp, the concentration of MB in the three samples decreased gradually. The calculated MB decomposition efficiency for V_2O_5 samples is: V_2O_5-CTAB: 62%, V_2O_5-P123: 80% and V2O5-SDS: 90%, respectively. Thus, V_2O_5-SDS exhibits better adsorption capacity than other two V_2O_5 samples. This phenomenon is due to the large surface area of the V_2O_5-SDS sample.

The adsorption-photocatalytic performance of V_2O_5 nanomaterial samples mainly depends on charge separation and surface morphology. According to first order kinetics reaction, rate constant k (min^{-1}) can be determined using the following equation:

$$Ln\left(\frac{C}{C_0}\right) = -kt \quad (6)$$

The first-order kinetics data for the photodegradation of MB on the prepared samples is shown in Fig. 8. All fitting curves of -ln(C/C) versus the irradiation time (t) are nearly linear. The rate constant of the catalysts obtained from the slope of the plots is given in Table 2. Here there is a difference in values due to the photocatalytic mechanism for decolorization of MB not only based on the generated OH radical but through a direct mechanism due to the relatively high surface area and hole-trapping sites.

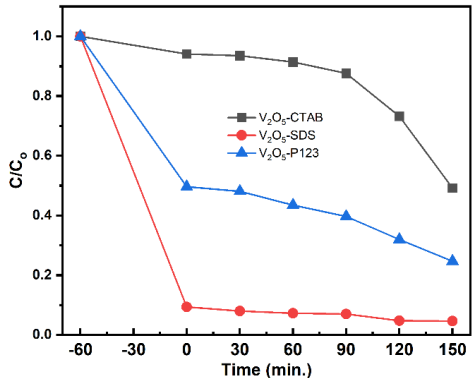

Fig. 7. The adsorption–photodegradation of MB solution using the synthesized V_2O_5 samples

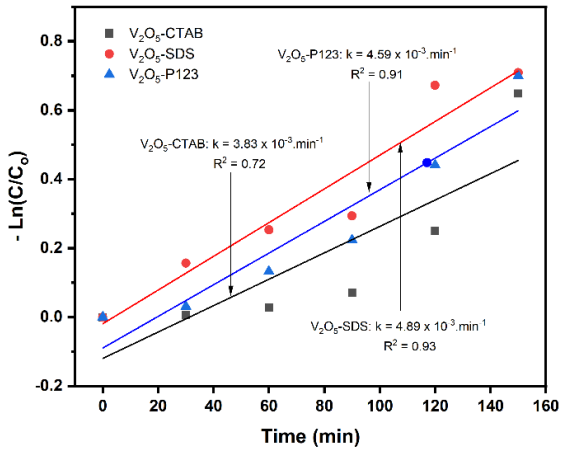

Fig. 8. -Ln(C/C$_0$) function of reaction time for the reduction of MB dye over nano vanadium oxide structures

Table 2. Pseudo first-order kinetics and adsorption efficiency of the samples

Sample ID	Rate constant (min^{-1})	R^2	Adsorption (%)
V_2O_5-CTAB	3.83×10^{-3}	0.72	5
V_2O_5-SDS	4.89×10^{-3}	0.93	95
V_2O_5-P123	4.59×10^{-3}	0.91	50

The degradation process could be described as following:

$$OH^- + h^+ \rightarrow {}^{\bullet}OH \quad (7)$$

$$V^{5+}(V_2O_5) + e^- \rightarrow V^{4+} \quad (8)$$

$$V^{4+} + O_2 \rightarrow V^{5+}(V_2O_5) + {}^{\bullet}O_2^- \quad (9)$$

$${}^{\bullet}OH + {}^{\bullet}O_2^- + \text{dye} \rightarrow \text{degradation products} + CO_2\uparrow + H_2O \quad (10)$$

When irradiated with light, electrons from the valence band (VB) of V_2O_5 are excited to the conduction band (CB) and leave holes in the VB. These holes will react with OH^- on the catalyst surface to form ${}^{\bullet}OH$ radicals, as seen in (7). The electrons after moving to the conduction band reduce a part of the V^{5+} ion to V^{4+} as in (8). The surrounding oxygen molecules will take electrons from V^{5+} to regenerate V^{4+} and superoxide anion radicals ${}^{\bullet}O_2^-$, as in (9). ${}^{\bullet}OH$ and ${}^{\bullet}O_2^-$ radicals are known to be the strongest oxidizing species and play an important role in the photocatalytic reaction efficiency [7]. On the other hand, hydroxy groups can trap holes due to their high electron density, and thus contribute to efficient carrier transfer from the interior to the surface of the material and prevent electron-hole recombination. In addition, the shape and size of the nanostructures also play an important role in enhancing the conact area between the photocatalyst and the pigment, thereby enhancing the photocatalytic efficiency.

In addition, the % degradation of MB was also compared with other photocatalysts in the literature (Table 3). It is clear that the V_2O_5 nanomaterials have much higher photocatalytic activity; therefore, they are very promising candidates for environmental remediation.

Table 3. Photodegradation of MB dye by different photocatalysts compared with literatures.

Photocatalyst	Weight of catalyst	Volume MB of solution	Initial MB solution concentration	Degradation time (min)	Light source	Photo degradation efficiency (%)	Ref.
MXene/g-C_3N_4	500 mg	100 ml	10 mg/L	180	Visible light (500W Halogen lamp)	69.4	[10]
N-doped $MnWO_4$	50 mg	100 ml	2.5×10^{-5} M	180	Visible light (300 W Tungsten lamp)	82	[11]
Fe_3O_4/ZnO	200 mg	50 ml	100 mg/L	120	Visible light (500 W Halogen lamp)	88.5	[12]
V_2O_5	30 mg	100 ml	20 mg/L	150	Visible light (120W Fluorescent lamp)	90	This work

4. Conclusion

We have successfully prepared V_2O_5 nanomaterials for catalytic applications. Different V_2O_5 nanostructures were synthesized by adding different surfactants (CTAB, SDS and P123) to the precursor solution. All samples exhibited similar optical and crystalline properties, with different morphologies. However, the sample V_2O_5-P123 formed rod structures with smaller size and higher porosity, indicating that significant effect of surfactants on the formation of morphologies of V_2O_5 nanostructures. Furthermore, sample V_2O_5-P123 exhibits higher photocatalytic efficiency than V_2O_5-CTAB; whereas the sample V_2O_5-SDS exhibits strong adsorption property for Methylene Blue dye solution. Our study suggests that by varying the surfactant we could control the morphology and catalytic activity of nanostructured V_2O_5 materials.

Acknowledgments

This research is funded by the Ministry of Science and Technology of Vietnam in Vietnam - Korea joint research program under the Grant no. NĐT/KR/21/20 and Hoa Lu University; and the Air Force Office of Scientific Research under award number FA2386-22-1-4043.

References

[1] Karthik Kannan, D. Radhika, A.S. Nesaraj, Mohammed Wasee Ahmed, R. Namitha, Cost-effective method of Co-doped rare-earth-based ceria (Y-CGO) nanocomposite as electrolyte for LT-SOFCs using CTAB as surfactant, Materials Research Innovations vol. 24, no. 7, 2020, pp. 414-421. https://doi.org/10.1080/14328917.2019.1706032

[2] Zhang X., Wang J.-G., Liu H., Liu H., Wei B., Facile synthesis of V_2O_5 hollow spheres as advanced cathodes for high-performance lithium-ion batteries, Materials, vol. 10, no. 1, Jan. 2017, pp. 77. https://doi.org/10.3390/ma10010077

[3] Hameed, Abdul & Khan, Muhammad Aslam & Ismail, Iqbal & Salah, Numan & Chandrasekaran, Sivaraman & Qamar, Muhammad, Evaluation of sunlight induced structural changes and their effect on the photocatalytic activity of V_2O_5 for the degradation of phenols, Journal of Hazardous Materials, vol. 286, Apr. 2015, pp. 127-135. https://doi.org/10.1016/j.jhazmat.2014.12.022

[4] Raj AT, Ramanujan K, Thangavel S, Gopalakrishan S, Raghavan N, Venugopal G., Facile synthesis of vanadium-pentoxide nanoparticles and study on their electrochemical, photocatalytic properties. J Nanosci Nanotechnol, vol. 15, no. 5, May. 2015, pp. 3802-8. https://doi.org/10.1166/jnn.2015.9543

[5] Ibrahim, Islam, George V. Belessiotis, Michalis K. Arfanis, Chrysoula Athanasekou, Athanassios I. Philippopoulos, Christiana A. Mitsopoulou, George Em. Romanos, and Polycarpos Falaras, Surfactant effects on the synthesis of redox bifunctional V_2O_5 photocatalysts, Materials, vol.13, no. 20, 2020, pp. 4665. https://doi.org/10.3390/ma13204665

[6] Shashank, M., Alharthi, F.A., Alsalme, A. et al., Ag decorated V_2O_5 nanorods as cathode material for lithium-ion battery, J Mater Sci: Mater Electron, vol. 31, 2020, pp. 14279–14286. https://doi.org/10.1007/s10854-020-03984-6

[7] Santhosh Kumar Jayaraj, Vishwanathan Sadishkumar, Thirumurugan Arun, Paramasivam Thangadurai, Enhanced photocatalytic activity of V_2O_5 nanorods for the photodegradation of organic dyes: A detailed understanding of the mechanism and their antibacterial activity, Materials Science in Semiconductor Processing, Vol. 85, 2018, pp. 122-133. https://doi.org/10.1016/j.mssp.2018.06.006

[8] Farahmandjou M, Abaeiyan N, Chemical synthesis of vanadium oxide (V_2O_5) nanoparticles prepared by sodium metavanadate, J Nanomed Res vol. 5, no. 1, 2017, pp. 00103. https://doi.org/10.15406/jnmr.2017.05.00103

[9] Jeghan Shrine Maria Nithya and Arumugam Pandurangan, Efficient mixed metal oxide routed synthesis of boron nitride nanotubes, RSC Adv., vol. 4, 2014, pp. 26697-26705. https://doi.org/10.1039/C4RA01204F

[10] Nasri MSI, Samsudin MFR, Tahir AA, Sufian S. Effect of MXene loaded on g-C_3N_4 photocatalyst for the photocatalytic degradation of methylene blue. Energies, vol. 15, no. 3, 2022; pp. 955. https://doi.org/10.3390/en15030955

[11] K. Sravan Kumar, Kammara Vaishnavi, Perala Venkataswamy, Gundeboina Ravi, Kadari Ramaswamy, Muga Vithal, Photocatalytic degradation of methylene blue over N-doped MnWO4 under visible light irradiation, Journal of the Indian Chemical Society, vol. 98, no. 10, 2021, pp. 100140. https://doi.org/10.1016/j.jics.2021.100140

[12] Rania Elshypany, Hanaa Selim, K. Zakaria, Ahmed H. Moustafa, Sadeek A. Sadeek, S.I. Sharaa, Patrice Raynaud, Amr A. Nada, Elaboration of Fe_3O_4/ZnO nanocomposite with highly performance photocatalytic activity for degradation methylene blue under visible light irradiation, Environmental Technology & Innovation, vol. 23, 2021, pp. 101710. https://doi.org/10.1016/j.eti.2021.101710